Technical Paper

ISSN 1997-1400 Int. J. Pavement Res. Technol. 4(3):131-139
Copyright @ Chinese Society of Pavement Engineering

In-situ Assessment of Stiffness During the Construction of HMA Pavements

Dharamveer Singh[1], Fares N. Beainy[2], Anh T. Mai[3], Sesh Commuri[4+], and Musharraf Zaman[5]

Abstract: Use of a newly developed intelligent compaction technology, called the Intelligent Asphalt Compaction Analyzer (IACA), to estimate the stiffness of an asphalt pavement during construction is addressed in this paper. The IACA is a neural network-based device that functions on the hypothesis that the roller and the underlying pavement layers form a coupled system and that the stiffness of the pavement layer can be determined through the vibration of the roller. For a given asphalt mix, the "Master Curves" for the dynamic modulus are first determined according to the AASHTO TP62-03 test method. During the compaction of the pavement, the IACA records the entire frequency spectrum of the vibrations of the roller and classifies these vibrations into different levels. The master curves are then used to calibrate the IACA to convert these levels of vibrations into a modulus value, representing the stiffness of the asphalt layer being compacted.

This two-step process produces stiffness measurements in real-time that are representative of the pavement being constructed. Also, since the neural network is calibrated during the construction of a stretch of the actual pavement, the stiffness measurements are obtained without the need to evaluate the underlying pavement layers and the subgrade. The IACA provides the stiffness values over the entire pavement in a non-destructive manner. Further, the proposed method allows for the verification of the estimated modulus through the falling weight deflectometer (FWD) or similar field tests of the constructed pavement.

Key words: *Asphalt stiffness; Dynamic modulus; Hot mix asphalt pavement; Intelligent compaction; In-situ measurement.*

Introduction

Stiffness is a key design factor that directly impacts the load bearing capacity of roadway pavements. Early deterioration of pavements due to rutting, fatigue cracking, and other types of distresses may be attributed to inadequate stiffness achieved during the compaction process [1]. The stiffness of a pavement is typically expressed in terms of its modulus, i.e., the relationship between the applied stress and the resulting deformation. The AASHTO 1993 mechanistic-empirical pavement design guide (MEPDG) [2] recognized the resilient modulus (M_R) as one of the primary mechanistic properties to evaluate performance of a pavement under vehicular loading and environmental conditions. Laboratory tests on the cyclic behavior of compacted hot mix asphalt (HMA) specimens show that their stress-strain relationships are temperature dependent. The National Cooperative Highway Research Program (NCHRP) Project I-37A recommends the use of dynamic modulus to characterize the HMA mixes [3]. With increased emphasis on the new mechanistic-empirical-based design procedures, predictive equations have been developed to estimate dynamic modulus of HMA layers as a function of such properties as mix type, aggregate structure, binder specifications, volumetric properties of compacted specimens, and mix temperature [4-8].

While dependence of the pavement performance on stiffness is well known, this parameter is rarely measured/monitored in the field during construction of a pavement. Instead, the current quality control (QC) methods in the field during construction of HMA pavements focus on the measurement of density of cores extracted from the finished pavement at specific locations. Unfortunately, the process of extracting roadway cores is destructive in nature and it often leads to the deterioration of the pavement. Also, remedial measures to rectify inadequate compaction problems after pavement has cooled down are costly and time consuming. Therefore, there is a need to develop cost effective techniques for rapid in-situ measurement and monitoring of pavement stiffness during the compaction process.

In-situ testing of mechanical properties of pavements and underlying subgrade soils is a widely researched area. Several test devices such as the Benkelman Beam, Lacroix Deflectograph, static plate loading test, and FWD are available for nondestructive evaluation of asphalt pavements [9-10]. More recently, the rolling weight deflectometer, spectral analysis of surface waves, and the Humboldt stiffness gauge have also been used to measure in-situ stiffness of pavement layers including subgrade [9, 11]. However, these test devices are applicable only after the compaction process is complete and pavement has cooled down to the ambient temperature. Therefore, although these tools can be used to identify deficiencies in compaction, they are not suitable for use during the construction of the pavement.

The need to measure the stiffness of a pavement during

1 Doctoral Candidate, School of Civil Engineering and Environmental Science, The University of Oklahoma, 202 West Boyd Street, Room 211, Norman, OK, 73019.
2 Doctoral Candidate, School of Electrical and Computer Engineering, The University of Oklahoma, 101 David L. Boren Blvd, Room 1050, Norman, OK, 73019.
3 Doctoral Candidate, School of Electrical and Computer Engineering, The University of Oklahoma, 101 David L. Boren Blvd, Room 1050, Norman, OK, 73019.
4 Associate Professor, School of Electrical and Computer Engineering, The University of Oklahoma, 101 David L. Boren Blvd, Room 1050, Norman, OK, 73019.
5 David Ross Boyd Professor and Aaron Alexander Professor, Associate Dean for Research, College of Engineering, The University of Oklahoma, 202 West Boyd Street, Room 107, Norman, OK, 73019.
+ Corresponding Author: E-mail scommuri@ou.edu
Note: Submitted April 6, 2010; Revised August 6, 2010; Accepted August 9, 2010

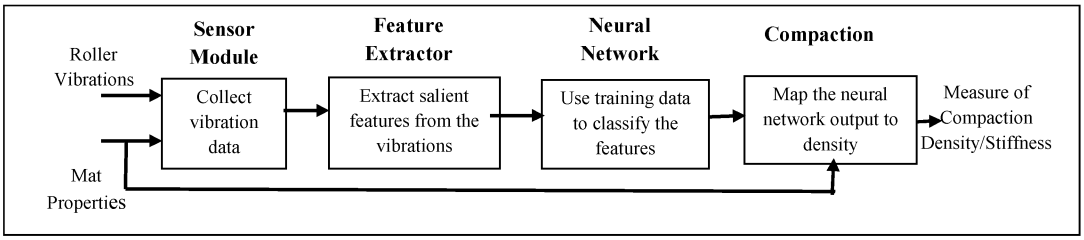

Fig. 1. Functional Schematic of the IACA [23].

construction has motivated the industry and equipment manufacturers to develop technologies that can ensure consistent and optimal compaction of HMA pavements [12-15]. Uniform compaction of both soil and aggregate bases is achieved through the variation of machine parameters such as amplitude and frequency of vibrations and vectoring of the thrust. Dynamic control of machine parameters allows for the application of the vibratory energy only to under-compacted areas and thereby preventing over-compaction and ensuring uniform compaction of subgrade soils and/or aggregate bases. While these intelligent compaction (IC) techniques hold promise, their performance is being evaluated by several Departments of Transportations (DOTs) and the Federal Highway Administration (FHWA) [16].

In contrast to the aforementioned intelligent compaction (IC) technologies [17-21], the IACA [22-24] is a measurement tool that analyzes, in real time, the vibrations of a vibratory compactor to estimate the level of compaction of a HMA mat or layer during construction. Use of IACA to estimate the density of asphalt pavements during construction was demonstrated previously [22-24].

In this paper, a calibration procedure is devised that will enable the IACA to estimate the stiffness of pavement during construction. The capability of the IACA is then demonstrated by comparing predicted stiffness data with the field data obtained from the constructed pavement. Specifically, FWD tests are performed at several locations on the constructed pavement and the measured stiffness is compared with the stiffness estimated by the IACA. It is shown that the IACA can estimate the stiffness of the pavement during construction with an accuracy suited for quality control in the field. The proposed IACA is expected to ensure uniform compaction, address under-compaction, and prevent over-compaction of the pavement.

Background on IACA

The IACA functions on the hypothesis that the vibratory roller and the underlying pavement layers form a coupled system. The response of the roller is determined by the frequency of its vibratory motors and the natural vibratory modes of the coupled system. Compaction of pavement increases its stiffness, and, as a consequence, the vibrations of the compactor are altered. The knowledge of the properties of the mat and the vibration spectra of the compactor can, therefore, be used to estimate the stiffness of the mat.

The functional modules in the IACA are schematically shown in Fig. 1. The sensor module (SM) in the IACA consists of accelerometers for measuring the vibrations of the compactor during operation, infrared temperature sensors for measuring the surface temperature of the asphalt mat being compacted, and a user interface for specifying the amplitude and frequency of the vibration motors and for recording the mix type and lift thickness. The feature extraction (FE) module computes the Fast Fourier Transform (FFT) of the input signal and extracts the features corresponding to vibrations at different salient frequencies. The Neural Network (NN) Classifier is a multi-layer NN that is trained to classify the extracted features into different classes where each class represents a vibration pattern specific to a pre-specified level of compaction. The compaction analyzer (CA) then post-processes the output of the NN and estimates the degree of compaction in real time.

The first step in the use of the IACA during compaction in the field is the determination of the vibration features of the roller and their correlation with the compaction levels achieved. In order to accomplish this goal, a 30-m long control strip is constructed first. The vibrations of the roller are measured using an accelerometer mounted on the axle of the drum. The power content in the vibration signals during each roller pass is then calculated, and the lowest and the highest power levels are determined [22-24]. Three equally spaced power levels between the lowest and the highest power levels are identified and the features corresponding to these five power levels are used to train the NN. During compaction, the NN observes the features of the roller vibration and classifies them into one of these five levels based on the levels of compaction that it is trained to recognize. Fig. 2 shows typical features corresponding to the five different compaction levels extracted from the spectrogram of the vibration signals. In this figure, the lowest level corresponds to the case where the roller is operating with the vibration motors turned off, and the highest level corresponds to the case where the maximum vibrations are observed. It is assumed that the characteristics of the underlying pavement layers do not vary extensively over the project extent. That is, any changes in the spectra of the vibrations are a result of the compaction achieved in the topmost asphalt layer. In case the properties of the underlying layers are not constant, then the IACA will have to be periodically recalibrated. As a practical matter, large variations in the properties of the underlying pavement layers are usually a result of pavement failure or insufficient site preparation. Even if the IACA is not recalibrated, these effects result in low compaction even after several roller passes and can easily be detected.

After the IACA is trained to classify the vibrations into estimated levels of compaction, it is calibrated to reflect the modulus of the pavement layer. In order to accomplish this, dynamic modulus tests for the mix used in the construction of the asphalt mat are performed according to the AASHTO TP 62-03 test method [25].

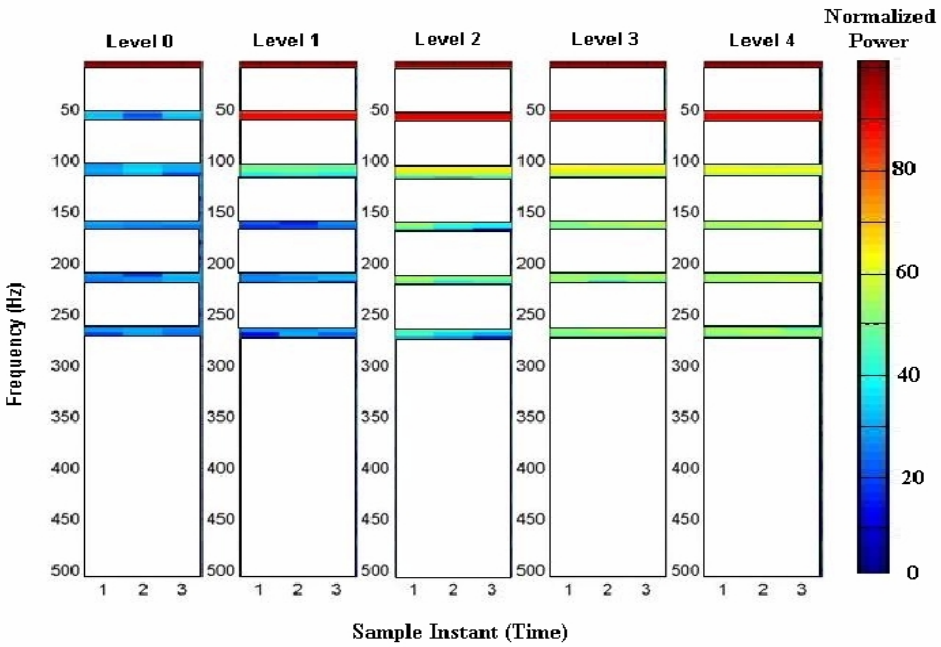

Fig. 2. Spectral Features Corresponding to Five Levels of Compaction.

From the Master Curves, the modulus value (M_T) at the target density of the compacted mix (from the mix design sheet) is noted. This modulus value is assumed to be the highest modulus that can be achieved during the compaction of the pavement. Likewise, the lowest modulus value observed, (M_{ld}), is assumed to correspond to the lay down density of the asphalt mat. The modulus estimated by the NN model, (M^i_{NN}), at location $P_i\ (i = 1,..,n)$, is then approximated as a linear relationship between the stiffness of the pavement and the observed levels of vibration.

$$M^i_{NN} = M_{ld} + k \times l^i_{NN} + off\,. \tag{1}$$

where, M^i_{NN}= modulus estimated by the neural network, k = slope, off = offset, and l^i_{NN} = compaction level estimated by the neural network. The initial slope is assumed to be equal to $(M_T - M_{ld})$/ (number of compaction levels), and the initial offset is set to zero.

The modulus estimated by the IACA after the initial calibration is based on the assumption that the target stiffness for the specified mix is indeed achieved during the compaction in the field. However, several factors, such as the compaction equipment, rolling pattern, lay down temperature of the mix, lift thickness, etc., influence the actual modulus of the pavement at any given location. In order to account for these deviations, measurements are taken using an FWD on the compacted pavement, and the slope and offset in Eq. (1) are recalculated to minimize the error between the estimated and measured values. If the modulus measured at location P_i is represented by M^i_{FWD}, then the measurement error is given by e_i and can be calculated as:

$$e_i = M^i_{NN} - M^i_{FWD} = M_{ld} + k \times l^i_{NN} + of\ f - M^i_{FWD}\,. \tag{2}$$

Minimizing the mean square error (MSE), one obtains the desired slope k.

$$k = \frac{\sum_{i=1}^{n}\left[\left(M^i_{FWD} - M^i_{ld} - off\right) \times l^i_{NN}\right]}{\sum_{i=1}^{n}\left(M^i_{NN}\right)^2} \tag{3}$$

The new offset is calculated as the mean error between the estimated and the measured stiffness, that is:

$$off = \frac{1}{n}\sum_{i=1}^{n}\left(M^i_{FWD} - M^i_{NN}\right) \tag{4}$$

Validation of the Stiffness Measurements

The procedure outlined above was demonstrated during the construction of a full depth pavement on Interstate I-35 in Norman, Oklahoma. This project involved the expansion of the existing alignment, stabilizing the subgrade to a depth of 200 mm using 10% cement kiln dust (CKD), followed by the installation of a 200-mm thick aggregate base. Two 100-mm thick asphalt layers, using an S3 mix (PG 64-22 OK), were then compacted on the top of this prepared base and then a third lift of 75 mm thickness was compacted using a 19-mm mix (S3, PG 76-28 OK). In the study reported in this paper, the IACA data were collected during the compaction of the third layer of this pavement. Since the construction was carried out at a fast pace, it was not possible to demonstrate the stiffness measurement for each asphalt layer separately. Measuring the stiffness only on the third layer implicitly assumes that the underlying pavement layers are of uniform stiffness. This assumption could possibly lead to variations in the estimated stiffness of the third layer. However, the results demonstrate that the technique proposed in this paper is suitable for

Table 1. Gradation and Properties of Collected Mix (S3 76-28).

Parameter	Value
25 mm Rock	22%
Manufactured Sand	50%
Sand	13%
R.A.P	15%
Asphalt Cement	PG 76-28 OK
G_{mm} (Maximum Specific Gravity of Mix)	2.523
G_{sb} (Bulk Specific Gravity of Aggregates)	2.657
G_{se} (Effective Specific Gravity of Aggregates)	2.677
% Asphalt	4.2
Specific Gravity of Asphalt	1.01

Mix Gradation	
Sieve Size (mm)	Percent Passing
25	100
19	98
12.5	87
9.5	80
4.75	62
2.36	40
1.18	27
0.6	20
0.3	12
0.15	5
0.075	2.8

Table 2. Mix Properties at Each Air Voids Levels (S3 76-28).

Parameter	Sample 1	Sample 2	Sample3
Target Air void (%)		6	
Actual Air void (%)	6.52	6.44	6.35
VMA (%)	14.96	14.89	14.81
VFA (%)	61.32	61.64	62.04
Target Air void (%)		8	
Actual Air void (%)	8.25	8.08	7.9
VMA (%)	16.54	16.38	16.21
VFA (%)	54.43	55.05	55.74
Target Air void (%)		10	
Actual Air void (%)	9.61	10.24	9.81
VMA (%)	17.78	18.34	17.96
VFA (%)	49.89	48.01	49.28
Target Air void (%)		12	
Actual Air void (%)	12.17	11.66	12.04
VMA (%)	20.11	19.64	19.98
VFA (%)	42.86	44.14	43.19

estimating the stiffness of the pavement during its construction. A systematic evaluation of the stiffness of each pavement layer is the focus of the ongoing research and will be reported after the study is completed.

Material Collection and Preparation of Test Specimen

The loose HMA mix used in the construction of the pavement layer (PG 76-28 OK) was collected from the construction site. The nominal maximum aggregate (primarily limestone) size was 19 mm. The mix contained approximately 22% rock, 50% manufactured sand, 13% sand, 15% recycled asphalt pavement (RAP), and 4.2% PG 76-28 OK binder. The gradations and other properties of the mix are summarized in Table 1.

The mix was preheated in an oven and compacted using a Superpave Gyratory Compactor (SGC). Four target air voids (6%, 8%, 10%, and 12%) were selected and three samples were compacted for each target air void. Samples that were 100 mm x 150 mm were then cored and sawed from the SGC compacted samples. The bulk specific gravity and air voids of the final specimens were determined as per AASHTO T166 [26]. Table 2 summarizes the target air voids, actual air voids, and other sample properties of final samples obtained in the laboratory. Dynamic modulus tests were then performed for each specimen according to the AASHTO TP62-03 test method [25].

Dynamic Modulus Testing

The dynamic modulus testing was done at four different temperatures, 4°C, 21°C, 40°C, and 55°C, starting at the lowest temperature and proceeding to the highest temperature. For each temperature level, the test was conducted at eight different frequencies from the highest to lowest, including 25 Hz, 10 Hz, 5 Hz, 1 Hz, 0.5 Hz, 0.1 Hz, 0.05 Hz, and 0.01 Hz. Prior to testing, the sample was conditioned by applying 200 cycles of load at a frequency of 25 Hz. The specimen was then placed in an environmental chamber and allowed to attain equilibrium at the specified test temperature (± 0.5%). The load magnitude was adjusted based on the material stiffness, air void content, temperature, and frequency to keep the strain response within 50-150 micro-strains. The data was recorded for the last five cycles of each sequence.

Construction of Master Curves

The master curves for different air voids levels (6%, 8%, 10%, and 12%) were generated at a reference temperature of 21°C using the procedure outlined in [27]. Eqs. (5) and (6) show the sigmoidal function and shift factor used for fitting the master curve. The default values of "A" and "VTS" for the PG76-28 binder were taken from AASHTO 2002 [3] as 9.200 and -3.024, respectively. A nonlinear optimization program was used for simultaneously solving these unknown parameters.

$$\log|E^*| = \delta + \frac{(Max-\delta)}{1+e^{\chi+\gamma\left[\log(f)+c\left(10^{(A+VTS\log T_R)}-\log\eta_{t=r}\right)\right]}} \quad (5)$$

The shift factor used here was of the following form:

$$a(T) = \frac{f_r}{f} \quad (6)$$

where, *Max* [in Eq. (5)] is the maximum E^* for a particular mix, f_r is the reduced frequency at reference temperature; f is the frequency at a particular temperature; $\eta_{t=r}$ is the viscosity of binder at reference temperature; A is the regression intercept of viscosity-temperature

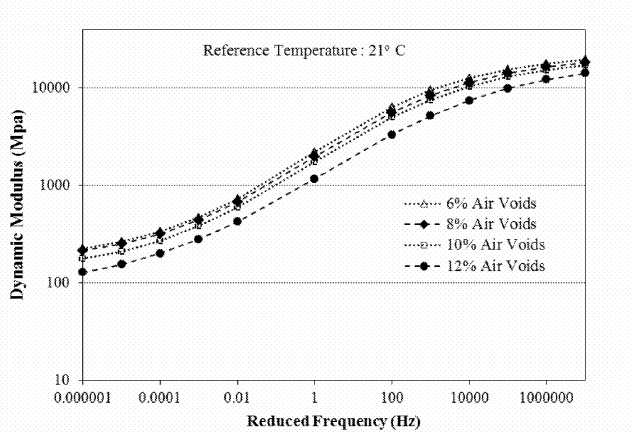

Fig. 3. Master Curves for Laboratory Measured Dynamic Modulus.

curve; *VTS* is the regression slope of viscosity-temperature susceptibility; $a(T)$ is the shift factor as a function of temperature and age; and δ, β, γ, and c are fitting parameters.

Results and Discussions

The dynamic modulus value was calculated at each of the frequencies and temperatures mentioned above. Therefore, a total of 32 dynamic modulus values were calculated (four temperature values × eight frequency values) for each test specimen. From these tests, the master curve was generated for each of the specified levels of air void. Following this approach, a total of 12 master curves (three samples at each target air voids) were constructed for the four selected target air void levels. The moduli of the three samples were averaged to obtain a single master curve representing the specific air void (Fig. 3). It can be seen from Fig. 3 that the dynamic modulus decreases as the air voids increase, as expected.

The "goodness-of-fit" statistic, S_e/S_y (standard error of the estimated/standard deviation), and correlation coefficient (R^2) were used to assess the validity of the correlation between laboratory measured and master curve fit equations [1]. Based on these criteria, the developed master curve equations in this study were found to be in excellent agreement with the laboratory measured data. The coefficients and the fitting statistics of the master curves are summarized in Table 3. The shift factor for all levels of air voids are calculated and tabulated in Table 4.

The master curves were used to determine the modulus at 12% and 6% air voids, i.e., corresponding to the lay down and target density for the asphalt mix. These values were used to calibrate the IACA as discussed in the previous section. During the construction of the 30-m long calibration stretch, three locations were marked (12 m, 15 m, and 18 m from the starting point of the stretch) along the center line of the lane. The estimated modulus was recorded at

Table 3. Master Curve Parameters for Laboratory Measured Dynamic Modulus for Mix S3 76-28.

Target Air Voids (%)	Sample No.	Actual Air Voids (%)	Max. E^*(MPa)	δ	β	γ	C	R^2	S_e/S_y	Correlation
6	1	6.52	22799	2.22	-0.08	-0.47	1.21	0.986	0.110	Excellent
	2	6.44	22835	2.24	-0.02	-0.50	1.24	0.988	0.154	Excellent
	3	6.35	22879	2.18	-0.20	-0.46	1.25	0.994	0.104	Excellent
8	1	8.25	21959	2.16	-0.03	-0.44	1.08	0.966	0.136	Excellent
	2	8.08	22042	2.23	0.07	-0.47	1.21	0.979	0.138	Excellent
	3	7.90	22131	2.31	0.02	-0.44	1.21	0.992	0.152	Excellent
10	1	9.61	21309	2.03	-0.11	-0.43	1.16	0.994	0.073	Excellent
	2	10.24	21013	2.21	0.16	-0.47	1.09	0.986	0.078	Excellent
	3	9.81	21215	2.03	-0.20	-0.44	1.02	0.992	0.114	Excellent
12	1	12.17	20109	1.88	0.05	-0.37	1.20	0.996	0.158	Excellent
	2	11.66	20348	1.88	-0.04	-0.39	1.17	0.996	0.103	Excellent
	3	12.04	20172	1.97	0.20	-0.43	1.03	0.991	0.093	Excellent

Table 4. Shift Factor for Laboratory Measured Dynamic Modulus for Mix S3 76-28.

Target Air Voids (%)	Sample No.	Actual Air Voids (%)	Shift Factor : log $a(T)$			
			4°C	21°C	40°C	55°C
6	1	6.52	2.189	0	-1.914	-3.125
	2	6.44	2.252	0	-1.969	-3.216
	3	6.35	2.268	0	-1.983	-3.239
8	1	8.25	1.950	0	-1.705	-2.784
	2	8.08	2.200	0	-1.923	-3.141
	3	7.90	2.182	0	-1.908	-3.116
10	1	9.61	2.103	0	-1.833	-3.002
	2	10.24	1.965	0	-1.718	-2.806
	3	9.81	1.853	0	-1.620	-2.646
12	1	12.17	2.167	0	-1.894	-3.094
	2	11.66	2.121	0	-1.854	-3.029
	3	12.04	1.873	0	-1.638	-2.675

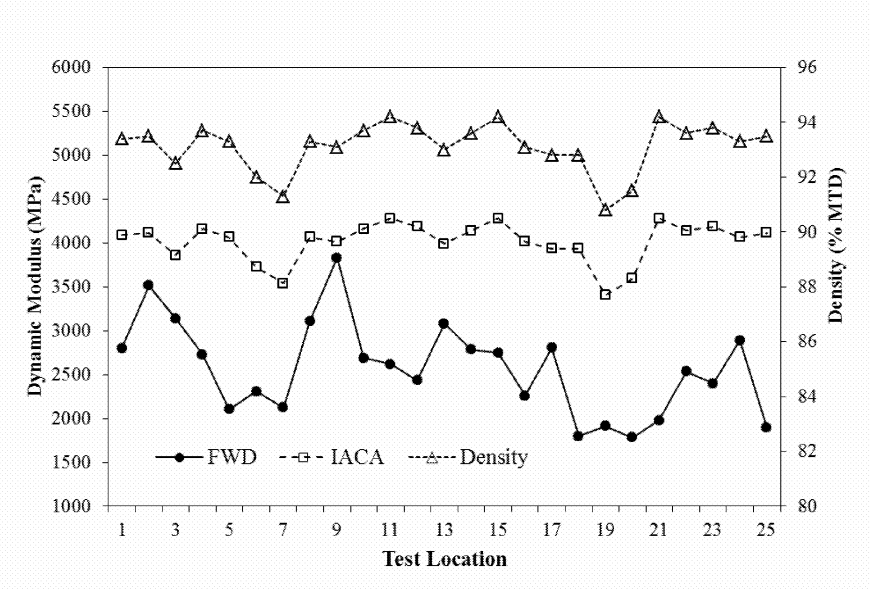

Fig. 4. Comparison of Estimated Modulus and FWD Measured Modulus at Locations on the Finished Pavement.

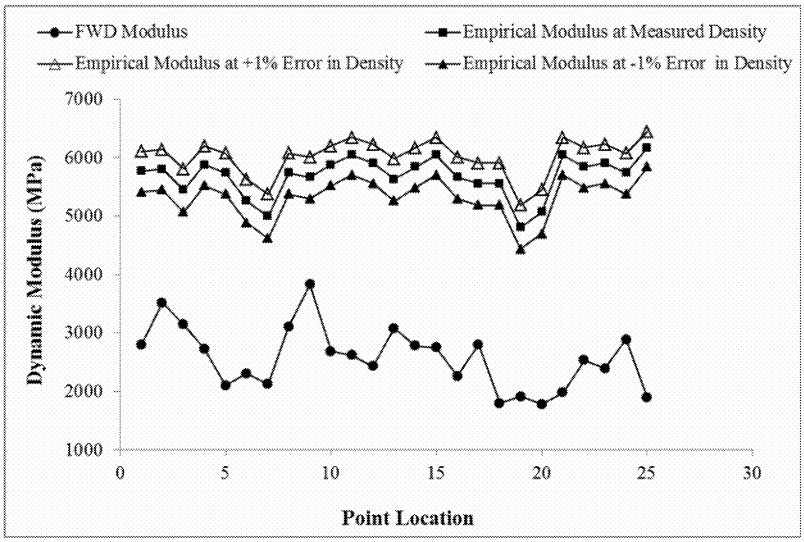

Fig. 5. Comparison of Empirical Modulus (20°C and 5 Hz) from Measured Density and FWD Measured Modulus at Locations on the Finished pavement.

these three locations after each roller pass. After the calibration stretch was completed, the asphalt mat was allowed to cool down to the ambient temperature and FWD tests were conducted at each of these three locations. The error between the measured and estimated modulus was used to recalibrate the IACA.

The proposed strategy was demonstrated during the construction of the 130-m long pavement. The estimated modulus over the entire pavement section was recorded during each roller pass. These data were then used to generate the modulus of the completed pavement. After the construction, the pavement was allowed to cool down to ambient temperature and FWD tests were conducted at 25 locations, approximately 5 m apart on the center of the compacted lane. The FWD loading induces a pulse of duration of 0.03 s [28], which is equivalent to a test frequency of 5.3 Hz ($1/0.03/2\pi$). Hence, the comparisons in this paper are performed using modulus values calculated at 21°C and 5 Hz frequency.

The estimated modulus and the FWD readings, as well as the estimated density at each of the 25 test locations, are shown in Fig. 4. The density measured at each of these locations by the IACA was also used to empirically calculate the modulus. Since it is known that the IACA measurements are typically within 1% of the density measured from pavement cores [24], the empirical modulus at each of these locations was also calculated using the Witczak 1999 model [8] at ±1% of the estimated density (Fig. 5).

It should be noted that the modulus measured by the IACA is the modulus of the third pavement layer while the FWD readings reflect the modulus of the entire multi-layered pavement. In order to compare the validity of the IACA estimates, four test locations, where the density [i.e., percent air voids (% AV)] data for each layer was avaliable, were selected. The density and the corresponding

Table 5. FWD and Laboratory Measured Effective Modulus.

Points	Laboratory Measured Modulus						Effective Modulus	FWD Modulus	Adj. Effective Modulus	Diff. FWD and Adj. Effective Modulus
	Base		2nd Layer		3rd Layer					
	AV(%)	(MPa)	AV(%)	(MPa)	AV(%)	(MPa)	(MPa)	(MPa)	(MPa)	(%)
T1N	8.1	5070	9.4	2659	7.1	3456	3658	2482	2624	5.71
T3N	6.7	5889	9.1	2751	7.7	3227	3865	2696	2772	2.81
T4N	8.3	4963	7.9	3155	7.9	3155	3750	2878	2689	-6.54
T5N	9.1	1556	7.7	3227	7.8	3191	3664	2657	2328	-1.09

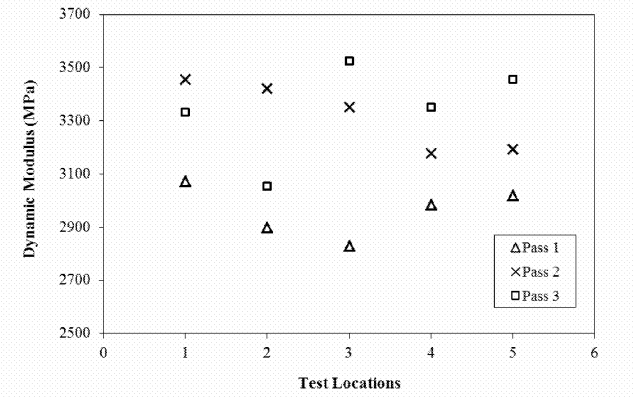

Fig. 6. Variation of Stiffness after Each Roller Pass at Five Equidistant Locations over the Length of the Pavement.

modulus at each of these locations are shown in Table 5. The effective layer density at each of these test locations was then calculated using the equivalent layer method [29-30]. The adjusted modulus in Table 5 is the equivalent field modulus mulitplied by the adjustement factor, where the adjustment factor is defined as the ratio of the average FWD readings and the average equivalent field modulus. It can be seen from Table 5 that the error between the adjusted layer modulus and the FWD measured modulus is within the accuracy range of the FWD device [31-33].

It is evident from Table 5 that the modulus estimated by the proposed method is in good agreement with the FWD measurements. The modulus calculated using the empirical methods, on the other hand, was significantly higher than the values measured by the FWD tests (Fig. 5). Further, the modulus estimated by the IACA reflects the density at each of these locations. However, the FWD readings show about 30% variation in the measured modulus for locations with approximately the same density. Changes in the stiffness at five locations on the pavement subjected to three roller passes are shown in Fig. 6. It can be seen that the modulus at three of these locations increased with a subsequent roller pass, while two other locations saw a reduction in the modulus from the second pass to the third pass. Such a reduction in the modulus values after roller passes at certain locations might be due to variation in the subgrade and inconsistency in the mix.

The method proposed in this paper requires prior computation of the dynamic modulus master curves for the asphalt mix being used in the construction. While such experimental testing might be time consuming, the master curves will have to be generated just once for each mix. There is significant research currently underway to develop models for the estimation of dynamic modulus based on data collected as part of the long term pavement performance (LTPP) project. In the future, it is expected that such master curves would be readily available for asphalt mixes that are commonly used across the country. If the primary goal during the field compaction is the uniformity of compaction, then approximate values of the stiffness at target and lay down densities can be used. While this would introduce a small error in the estimated stiffness, such approximate measurements can eliminate the need for conducting dynamic modulus tests. The results in this paper also highlight the critical areas for future investigations. One of the observations during the field tests was the high variability in FWD data at locations having similar compaction. Future tests are planned to first determine the stiffness of the subgrade and study its impact on the stiffness obtained after the compaction of the HMA layer(s). Tests are also underway to determine the repeatability and accuracy of the FWD measurements.

Concluding Remarks

A neural network-based technique to determine the stiffness of a pavement layer during its construction was demonstrated in this paper. The vibrations of the compactor are used to determine the level of compaction that is achieved. These levels of compaction are then converted into a modulus value. The two-step calibration process developed in this paper produces stiffness measurements in real-time that are representative of the pavement being constructed. Also, since the neural network is calibrated during the construction of a stretch of the actual pavement, the stiffness measurements are obtained without the need to evaluate the underlying pavement layers and the subgrade. The IACA provides the stiffness values over the entire pavement in a non-destructive manner. Further, the proposed method allows for the verification of the estimated modulus through FWD or similar field tests of the constructed pavement. It is seen that empirical calculations of the modulus from the laboratory data provide significantly higher values of the modulus and may not be suited for quality control purposes during compaction. On the other hand, the IACA can estimate the modulus in real-time during the compaction process and can be used to ensure uniform compaction of the asphalt pavement. A systematic evaluation of the stiffness of each pavement layer is the focus of the ongoing research.

Acknowledgments

This work was funded through grants from the Highways for Life Program, FHWA, Washington DC; Volvo Construction Equipment Company, Shippensburg, PA; and the Oklahoma Transportation Center (OTC).

The authors wish to thank Eric Weaver, research highway engineer, FHWA Office of Infrastructure R&D, McLean, Virginia, and Victor Gallivan, asphalt pavement engineer, FHWA Office of Pavement Technology, Indianapolis, Indiana, for their numerous suggestions and assistance during this project. The authors also wish to express their sincere gratitude to Haskell Lemon Construction Company, Oklahoma City, Oklahoma, for their assistance during every phase of this project.

References

1. Pellinen, T.K., and Witczak, M.W., (2002). Use of Stiffness of Hot-Mix Asphalt as a Simple Performance Test, *Transportation Research Record*, No. 1789, pp. 80-90.
2. AASHTO (1993). AASHTO Guide for Design of Pavement Structures, American Association of State Highway and Transportation Officials (AASHTO), Washington, D.C.
3. AASHTO (2002). Guide to the Mechanistic-Empirical Design of New and Rehabilitated Pavement Structures, *NCHRP-1-37A*, Chapter 2, pp. 1-81, http://www.trb.org/mepdg/guide.htm,Last Accessed March, 10, 2008, Washington, DC.
4. Ayres, M., Jr., and Witczak. M.W. (1998). AYMA - A Mechanistic Probabilistic System to Evaluate Flexible Pavement Performance, *Transportation Research Record*, No. 1629, pp. 137-148.
5. Crovetti, J., Hall, K.T., and Williams, C., (2005). Development of Modulus to Temperature Relations for HMA Mixtures Used in Wisconsin, Final Report, Wisconsin Highway Research Program # 0092-03-14, Wisconsin Department of Transportation, pp. 45-65, Madison, WI.
6. Katicha, S.W., (2003). Development of Laboratory to Field Shift Factors for Hot Mix Aspahlt Resilient Modulus, M.S. Thesis, Virginia Polytechnic Institute and State University, pp. 56-89, Blacksburg, VA.
7. Tarefder, R.A., (2003). Laboratory and Model Prediction of Rutting in Asphalt Concrete, Ph.D. Dissertation, University of Oklahoma, pp. 128-157, Norman, OK.
8. Andrei, D., Witczak, M.W., and Mirza, M., (1999). Development of Revised Predictive Model for the Dynamic Complex Modulus of Asphalt Mixtures, *NCHRP 1-37A*, Interim Report NCHRP 1-37 A, Deptartment of Civil Engineering, University of Maryland, College Park, MD.
9. Newcomb, D. and Birgisson, B., (1999). Methods for Measuring In Situ Subgrade Mechanical Properties of Pavement Subgrade Soils, *NCHRP Synthesis 278*, Transportation Research Board, pp. 24-42, Washington, DC.
10. Tayabji, S. and Lukanen, E., (2000). Nondestructive Testing of Pavements and Backcalculation of Moduli, *ASTM STP 1375*, ASTM International, pp.72-94.
11. Navaratnarajah, S.K., (2006). "Performance Characteristics of Selected Asphalt Mixes: A Laboratory and Field Study," Thesis submitted to the School of Civil Engineering and Environmental Science, University of Oklahoma, pp. 56-85, Norman, Oklahoma.
12. Camargo, F., Larsen, B., Chadbourn, B., Roberson, R., and Siekmeier, J., (2006). Intelligent Compaction: A Minnesota Case History, presented at *the 54th Annual University of Minnesota Geotechnical Conference*, Minnesota, USA.
13. Landers, K., (2006). The World of Smart Compaction Systems, *Better Roads*, 76(10), pp. 56-59.
14. Moore, W., (2006). Intelligent Compaction: Outsmarting Soil and Asphalt, *Construction Equipment*, Vol. 4, pp. 39-48.
15. Petersen, D. L., (2005). Continuous Compaction Control, Mn-ROAD Demonstration, *Report: MN/RC – 2005-07*, submitted to Federal Highway Administration, pp. 3-13, St. Paul, MN.
16. FHWA (2009). Accelerated Implementation of Intelligent Compaction Technologies for Embankment Subgrade Soils, Aggregate Bases, and Asphalt Materials, US FHWA Research Project DTFH61-07-C-R0032. http://www.intelligentcompaction.com, Last Accessed November 28, 2009.
17. Ammann (2009). Is the Soil Compacted Enough? http://www.ammann-group.com/en/technology/intelligent-ground-compaction/ (last accessed February 22, 2011).
18. Bomag (2009). Systems for Soil and Asphalt Compaction. http://www.bomag.com/americas/ (last accessed February 22, 2011).
19. Caterpillar (2009). Intelligent Compaction: A Developing Technology.http://www.cat.com/cda/components/fullArticle?m=312616&x=7&id=927320. (last accessed February 22, 2011).
20. Geodynamik (2009). The First Step to More Effective Roller. http://www.geodynamik.com/languages/english/index_gb.html. (last accessed February 22, 2011).
21. Sakai (2009). Intelligent Compaction System Proving Success . http://www.prweb.com/releases/SAKAI/IntelligentCompaction/prweb2712524.htm (last accessed February 22, 2011).
22. Commuri, S., and Zaman, M., (2008). A Novel Neural Network-Based Asphalt Compaction Analyzer, *International Journal of Pavement Engineering,* 9(3), pp. 177-188.
23. Commuri, S., Mai, A.T., and Zaman, M., "Neural Network-based Intelligent Compaction Analyzer for Estimating Compaction Quality of Hot Asphalt Mixes," *ASCE Journal of Construction Engineering and Management*, January 2011 (online) (http://scitation.aip.org/getabs/servlet/GetabsServlet?prog=normal&id=JCEMXX000001000001000239000001&idtype=cvips&gifs=yes).
24. Commuri, S., Mai, A., and Zaman, M., (2009). Calibration Procedures for the Intelligent Asphalt Compaction Analyzer, *ASTM Journal of Testing and Evaluation*, 37(5), pp. 454-462.
25. American Association of State Highway and Transportation Officials (AASHTO), (2006). Standard Method of Test for Determining Dynamic Modulus of Hot-Mix Asphalt Concrete Mixtures: TP62-03, AASHTO Provisional Standards.
26. American Association of State Highway and Transportation Officials (AASHTO), (2006). Standard Method of Test for Bulk Specific Gravity of Compacted Bituminous Mixtures Using Saturated Surface Dry Specimens: T166.
27. Bonaquit, R. and Christensen, D.W., (2005). Practical Procedure for Developing Dynamic Modulus Master Curves for Pavement Structural Design, *Transportation Research Record*, No. 1929, pp. 208-217.

28. Loulizi, A., Al-Qadi, I.L., Lahouar, S., and Freeman, T.E., (2002). Measurement of Vertical Compressive Stress Pulse in Flexible Pavements and Its Representation for Dynamic Loading Tests, *Transportation Research Record*, No. 1816, pp. 125-136.
29. Lu, Q., Ullidtz, P., Basheer, I., Ghuzlan, K., and Signore, J.M., (2009). CalBack: Enhancing Caltrans Mechanistic-Empirical Pavement Design Process with New Back-Calculation Software, *Journal of Transportation Engineering*, 135(7), pp. 479-488.
30. Shalaby, A., Liske, T., and Kavussi, A., (2004). Comparing Back-Calculated and Laboratory Resilient Moduli of Bituminous Paving Mixtures. *Canadian Journal of Civil Engineering*, Vol. 31, pp. 988-996.
31. Gedafa, D.S., Hossain, M., Romanoschi, S.A., and Gisi, A.J., (2010). Comparison of Moduli of Kansas Superpave Asphalt Mixes, 89th Annual Transportation Research Board Meeting, Washington, DC.
32. Hossain, M., and Scofield, L., (1992). Correlation Between Backcalculated and Laboratory-Determined Asphalt Concrete Moduli, *Transportation Research Record*, No. 1377, pp. 67-76